

# Direct-printing fabrication and characterization of rGO-CuS buckypaper electrode for supercapacitor

Doan Thanh Tung<sup>1,2,\*</sup>, Le Thi Thanh Tam<sup>1,2</sup>, Hoang Tran Dung<sup>1</sup>, Nguyen Thi Yen<sup>1</sup>,  
Ngo Ba Thanh<sup>1</sup>, Ngo Thanh Dung<sup>1</sup>, Le Trong Lu<sup>1,2,\*</sup>

<sup>1</sup>*Institute for Tropical Technology, Vietnam Academy of Science and Technology,  
18 Hoang Quoc Viet, Cau Giay, Ha Noi, Viet Nam*

<sup>2</sup>*Graduate University of Science and Technology, Vietnam Academy of Science and Technology,  
18 Hoang Quoc Viet, Cau Giay, Ha Noi, Viet Nam*

\*Emails: [ltlu@itt.vast.vn](mailto:ltlu@itt.vast.vn); [dtungnt167@gmail.com](mailto:dtungnt167@gmail.com)

Received: 31 October 2022; Accepted for publication: 30 January 2023

**Abstract.** In this study, Buckypaper (BP) is fabricated by vacuum filtering method, used as a current collector for supercapacitors (SC). This BP is then directly printed with rGO-CuS hybrid nanomaterial ink onto its surface via a custom 3D printer. The structure of material components is characterized using transmission electron microscopy (TEM), energy-dispersive X-ray spectroscopy (EDS) and scanning electron microscopy (SEM). Also, electrochemical impedance spectroscopy (EIS), cyclic voltammetry (CV) and galvanostatic charge-discharge (GCD) analyses are conducted to estimate the electrochemical performance. The results show that the fabricated SC electrode is of good quality with a specific capacitance of 680.9 F/g at a scan rate of 5 mV/s. Besides, the electrode also has characteristic redox peaks and a stability of 94.3 % after 6000 discharges at a current density of 25 A/g.

**Keywords:** electrode, nanomaterials, supercapacitors, 3D printer, sulfide metal, graphene.

**Classification numbers:** 2.4.4, 2.8.2

## 1. INTRODUCTION

Sumio Iijima was the first scientist to discover carbon nanotubes (CNTs) materials and their structure in 1991 [1]. Since then, carbon nanotubes have gained remarkable research interest owing to their special mechanical - thermal - electrical properties and have an extensive range of potential applications in various sectors, such as aerospace, automobile, biomedical, defense, energy, etc. [2 - 4]. The Young's modulus for individual MWCNTs of between 0.27 - 0.95 TPa and strengths in the 11 - 63 GPa range were reported by Byrne and Gun'ko [5]. These make CNTs the strongest and stiffest materials on earth. However, carbon nanotubes are very tiny, with diameters as small as 1 nm and a few micrometers long. The nanoscale makes carbon nanotubes practically of little use for industrial purposes alone, so many methods have been developed to fabricate the macroscopic lattice of carbon nanotubes. Carbon nanotube lattices,

also known as Buckypaper, have been shown to have better mechanical, thermal and electrical properties than individual CNTs. To make Buckypaper, the CNTs dispersion is a necessary step. However, CNT agglomeration has always happened and is a problem that needs to be fixed [6]. The CNTs tend to aggregate and form clusters owing to high van der Waals force between the tubes ( $\pi$ - $\pi$  stacking interaction), so the solubility in common solvents (e.g.  $H_2O$ , alcohol, N,N-dimethylformamide (DMF), etc.) and the interaction between CNTs and other compounds such as polymeric matrix or molecules are very limited. Unfortunately, this aggregation results in inefficient stress transfer to individual nanotubes and tends to reduce the mechanical properties of modified membranes [7, 8].

Although CNTs in general and BP in particular are not completely new topics, they are still of interest to research by many scientists, especially in the field of energy storage [9-13]. Popov and his associates produced BP by filtering acidic suspensions of multiwalled CNTs (MWCNTs) through polyester membranes without using a binder [14]. The fabricated supercapacitor electrode had the best specific surface area of  $66\text{ m}^2/\text{g}$  and specific capacitance ( $C_s$ ) of  $25\text{ F/g}$  at a scan rate of  $20\text{ mV/s}$  with  $6\text{ M KOH}$  electrolyte. When CNTs were combined with activated carbon, CNT/AC gave a larger capacitance value of  $135.2\text{ F/g}$  at a current density of  $1.0\text{ A/g}$  [15]. The pure-carbon electrodes only have a double layer charge effect, so the theoretical capacitance value is not high. Therefore, the additional use of materials that contribute to the pseudo-capacitance effect through reversible oxidation-reduction reactions is necessary. Yi-Hsuan Lai *et al.* incorporated NiO into CNT to make composite electrode materials in paper form. The hybrid paper electrode showed a high specific capacitance of  $713.9\text{ F/g}$  at a scan rate of  $2\text{ mV/s}$  [16]. In addition, conductive polymer materials such as polyaniline (PANi) and polypyrrole (PPy) have also been studied for different customized forms of BP [17, 18].

Our recent studies favor metal sulfide materials because they have high capacitance values up to thousands of  $\text{F/g}$  [19 - 22]. Therefore, in this study, we fabricated supercapacitor electrodes by directly printing of rGO-CuS nano-hybrid ink onto the BP surface. The BP construction process was calibrated with the goal of minimizing surfactants as well as binders. And it acted as a substrate or current collector. The analytical results show that the fabricated SC electrode is of good quality with a specific capacitance of  $680.9\text{ F/g}$  at a scan rate of  $5\text{ mV/s}$  and a stability of  $94.3\%$  after 6000 discharges at a current density of  $25\text{ A/g}$ .

## **2. MATERIALS AND EXPERIMENTAL**

### **2.1. Materials**

CNTs were synthesized by the Laboratory of Carbon Nanomaterials using chemical vapor deposition. Graphene oxide (GO) was synthesized by the Center for Advanced Materials Development using a modified Hummer method.

Copper (II) sulfate pentahydrate  $\geq 98\%$  ( $\text{CuSO}_4 \cdot 5\text{H}_2\text{O}$ ), 1-Dodecanethiol (DDT)  $98\%$ , oleylamine (OLA)  $70\%$ , octadecene, nitrosonium tetrafluoroborate ( $\text{NOBF}_4$ ), polyvinyl alcohol (PVA), sodium dodecyl sulfate (SDS), Triton X-100, ethanol, isopropanol, acetone, hexane, chloroform, and potassium hydroxide (KOH) were purchased from Sigma-Aldrich. All chemicals were used as received without further purification.

### **2.2. Experimental**

Figure 1 shows the schematic diagram of the rGO-CuS/Buckypaper supercapacitor electrode fabrication process. This process consists of three main stages:

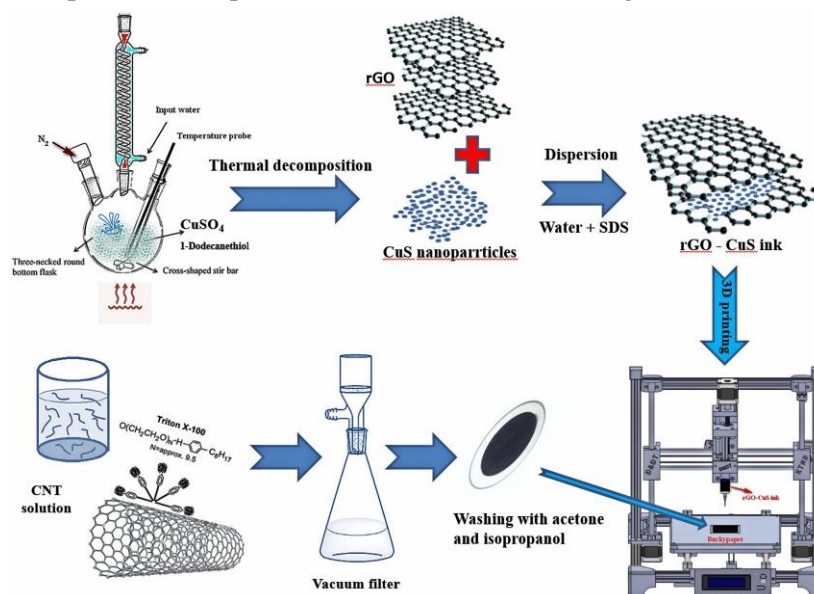


Figure 1. Schematic illustration of the rGO-CuS/Buckypaper electrode fabrication process.

### 2.2.1. Preparation of MWCNT buckypaper

MWCNT was fabricated by CVD method and the finished product was black fine powder. During heating at 80 °C, 100 mg of MWCNT was dispersed in 200 mL of double distilled water with simultaneous support of 2 mL of Triton X-100 surfactant by a magnetic stirrer. When the solution was relatively homogeneous, the suspension was ultrasonically vibrated for 2 h. Then, the solution was put into a vacuum filtration system to form a membrane with 0.45 µm nylon filter paper. This filtering process took several hours. The prepared bucky paper was naturally dried for 24 h. And it was washed with a mixture of acetone and isopropanol to remove the surfactant. Finally, the buckypaper was used as a conductive substrate for the supercapacitor printing process.

### 2.2.2. Fabrication of rGO-copper sulfide ink

**Synthesis of CuS nanoparticles (NPs):** CuS NPs were prepared using a modified thermal decomposition method as previously reported [23, 24]. In a typical synthesis, 7.5 g of  $\text{CuSO}_4 \cdot 5\text{H}_2\text{O}$ , 4 mL of 1-DDT as a sulfur source and 2 mL of OLA as a surfactant were mixed with 30 mL of octadecene in a three-neck round bottom flask and evacuated at room temperature for 20 min. The mixture was continuously magnetically stirred while the temperature of the three-neck flask was raised to 100 °C and kept for 30 min. The reaction mixture was then heated to 200 °C for 60 min and to 240 °C for another 60 min. The solution was allowed to cool to room temperature. The CuS NPs were washed several times with a mixture of n-hexane and ethanol, then centrifuged at 12000 rpm for 3 min to obtain a black product. Finally, NOBF<sub>4</sub> was used as an exchange ligand to modify the surface of CuS NPs in chloroform solution [24]. Currently, the CuS NPs have the ability to disperse in a polar and hydrophilic solvent such as water, alcohol, DMF, etc.

**rGO-CuS ink:** The graphene oxide (GO) synthesized using a modified Hummer method was calcined at 460 °C for 30 min to reduce GO [25]. The reduced graphene oxide (rGO) and SDS were dispersed in double distilled water at a concentration of 20 mg/mL. For good dispersion, the rGO/SDS ratio was about 5/3 [26]. The process of sequentially adding CuS nanoparticles with a concentration of 3 mg/mL and PVA as a binder with a concentration of 2 mg/mL into the rGO suspension was carried out using continuous magnetic stirring and heating at 80 °C. When the rGO-CuS mixture was relatively homogeneous, it was ultrasonically vibrated for 2 h and stirred overnight.

### *2.2.3. Inkjet printing of supercapacitor electrodes*

Buckypaper was spread flat on the printer's heat bed at a temperature of 80 °C to make the printing conductive substrate. The electrode printing and fabrication process was carried out as in our previous publication [24]. The supercapacitor electrode was then heat treated at 300 °C under N<sub>2</sub> gas conditions.

## **2.3. Characterisations**

The morphology and the elemental composition of Buckypaper and printed rGO-CuS film were observed by scanning electron microscopy (SEM-EDX Jeol JSM-6510LV). The transmission electron microscopy (TEM, Jeol JEM-1010 microscope) was used to investigate the morphology of the synthesized CuS nanoparticles.

The electrochemical properties of the printed rGO-CuS/BP electrodes were characterized by a Bio-Logic VSP-300 electrochemical station. A three-electrode electrochemical bath consisted of a standard calomel electrode (SCE) as a reference electrode (RE), a 1.5 cm × 1.7 cm platinum plate as a counter electrode (CE), the rGO-CuS/BP electrodes as working electrodes (WE) with an active surface area of 2 cm × 1 cm and 6 M KOH as an electrolyte. The electrode samples were immersed in the electrolyte solution for about 30 min, then the measurements such as cyclic voltammetry (CV), galvanostatic charge/discharge (GCD), and electrochemical impedance spectroscopy (EIS) were performed. Different CV scan rates of 5, 10, 20 and 50 mV/s were applied over the voltage range from -1 V to -0.1 V. With the same potential range, the rGO-CuS/BP electrodes were charged/discharged by the GCD method with different current densities (1, 2, 4, 6 and 10 A/g). The electrochemical impedance spectroscopy (EIS) test was performed in the frequency range of 0.1 Hz - 200 kHz. Finally, the GCD process was repeated several times with a current density of 25 A/g to evaluate the durability of the supercapacitor electrodes.

## **3. RESULTS AND DISCUSSION**

### **3.1. Material characterization**

To play the role of the SC current collector, BP needs to have a relatively good mechanical strength. With the amount of MWCNT increased to 100 mg for a single vacuum filtration, the BP produced has an average thickness in the range of 200 - 300 μm (Fig. 2a). The carbon nanotubes are compressed by the vacuum pump causing them to squeeze together and intertwine. Figure 2b presents the SEM image of the Buckypaper's surface. It shows that CNTs with a diameter much smaller than their length are spread out in many stacked layers. The Triton X-100 surfactant removed from good-length CNTs by a mixture of acetone and isopropanol will help achieve better conductivity.

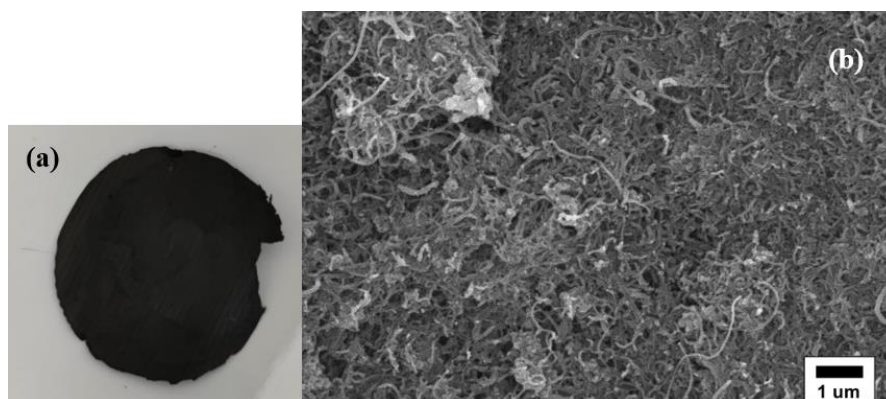


Figure 2. (a) Buckypaper and (b) its SEM image.

Once the conductive substrate was in place, ink preparation requires uniform dispersion of all its components. Nanoparticles of small and similar size will easily disperse evenly in the solution [20, 24]. TEM image and size distribution of CuS nanoparticles are shown in Fig. 3. According to the results of random diameter measurements of 266 CuS nanoparticles, the average diameter is 6.5 nm. Thus, the CuS nanoparticles synthesized by this organic solvent thermal decomposition method have a very small size and are relatively uniform.

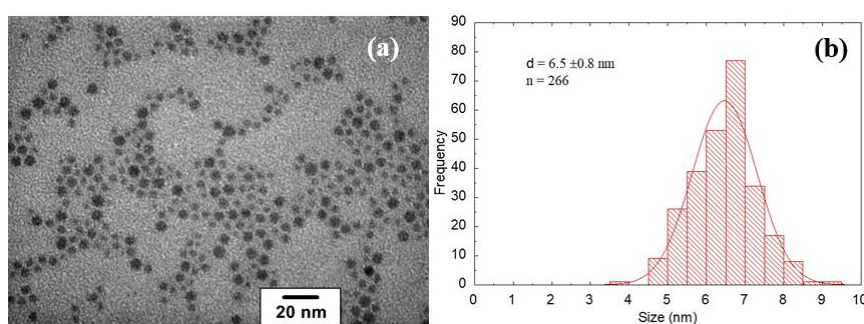


Figure 3. (a) TEM image and (b) size distribution of CuS.

After the surface of the CuS nanoparticles was modified with  $\text{NOBF}_4$ , they still had small size, so they were easily dispersed in aqueous solvents. The fabricated rGO-CuS ink is shown in Fig. 4a. The ink was then coated onto the BP paper with an area of 2 cm x 1 cm for the SC electrode sample (Fig. 4b). Thanks to the PVA polymer binder and the roughness of the Buckypaper, the printing process went smoothly with good adhesion. Figure 4c and Fig. 4d show SEM images of rGO-CuS electrode surface without heat treatment and with heat treatment at 300 °C under  $\text{N}_2$  gas conditions. For supercapacitor electrode without heat treatment, its surface is rich in SDS surfactant along with PVA binder. As for the calcined electrode, on its surface, graphene sheets and some clusters of particles clinging to the surface can be clearly seen. This can be explained by the fact that SDS and a part of PVA degrade at temperatures between 200 and 300 °C [27]. The initial amount of SDS present in the ink is relatively large with the rGO/SDS ratio of 5/3. Therefore, the calcination process at 300 °C under  $\text{N}_2$  gas conditions with suitable time will help remove the surfactants. And it is necessary to improve the conductivity as well as the contact ability of the electrode with the electrolyte solution.

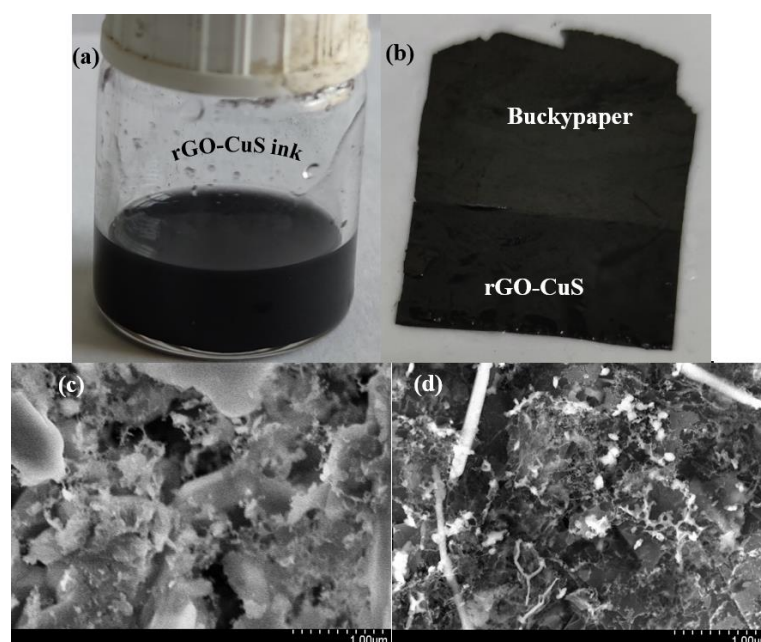


Figure 4. (a) rGO-CuS ink, (b) rGO-CuS/BP SC electrode, (c) SEM image of the printing SC electrode without heat treatment and (d) with annealing at 300 °C under N<sub>2</sub> gas condition.



Figure 5. EDS analysis of rGO-CuS SC electrode.

EDS allows the analysis of elements on the surface of the printed electrode. With a background of Bucky paper and graphene, the carbon content is the majority. Even so, the elements Cu and S also appear and have characteristic peaks in Fig. 5. The elemental compositions of SDS and PVA contain elements Na, S and O, so they are also present in this analysis. Thus, the CuS nanoparticles are distributed in rGO material with the goal of increasing the redox effect and electrochemical quality of the supercapacitor.

### 3.2. Electrochemical measurements

The EIS analysis was performed in order to evaluate the charge transport behavior of the printed rGO-CuS electrodes. All the ESR measurements were conducted in a frequency range of



0.1 Hz - 200 kHz. The results of the EIS analysis are represented as a Nyquist plot in Fig. 6a. It is composed of a high-frequency region (semicircles) and a low-frequency region (straight-looping lines). The intersection of the high-frequency region with the  $\text{Re}(Z)$  axis represents the ESR of the electrochemical system, caused by the internal resistance of the electrode and the resistance of the electrode-electrolyte interface. According to the graph (Fig. 6a), the ESR has a value of about  $1.5 \Omega$ , which shows that the resistance of BP and rGO-CuS materials is not too high. The diameter of the semicircles indicates that the Faradaic charge-transfer resistance ( $R_{ct}$ ) of the electrode material has a value of about  $0.2 \Omega$ . Very low  $R_{ct}$  indicates high ion exchange capacity and is favorable for reversible redox reactions. At low frequencies, the straight-looping lines show the diffusion resistance (Warburg resistance,  $W$ ) of the electrolyte ions [24].

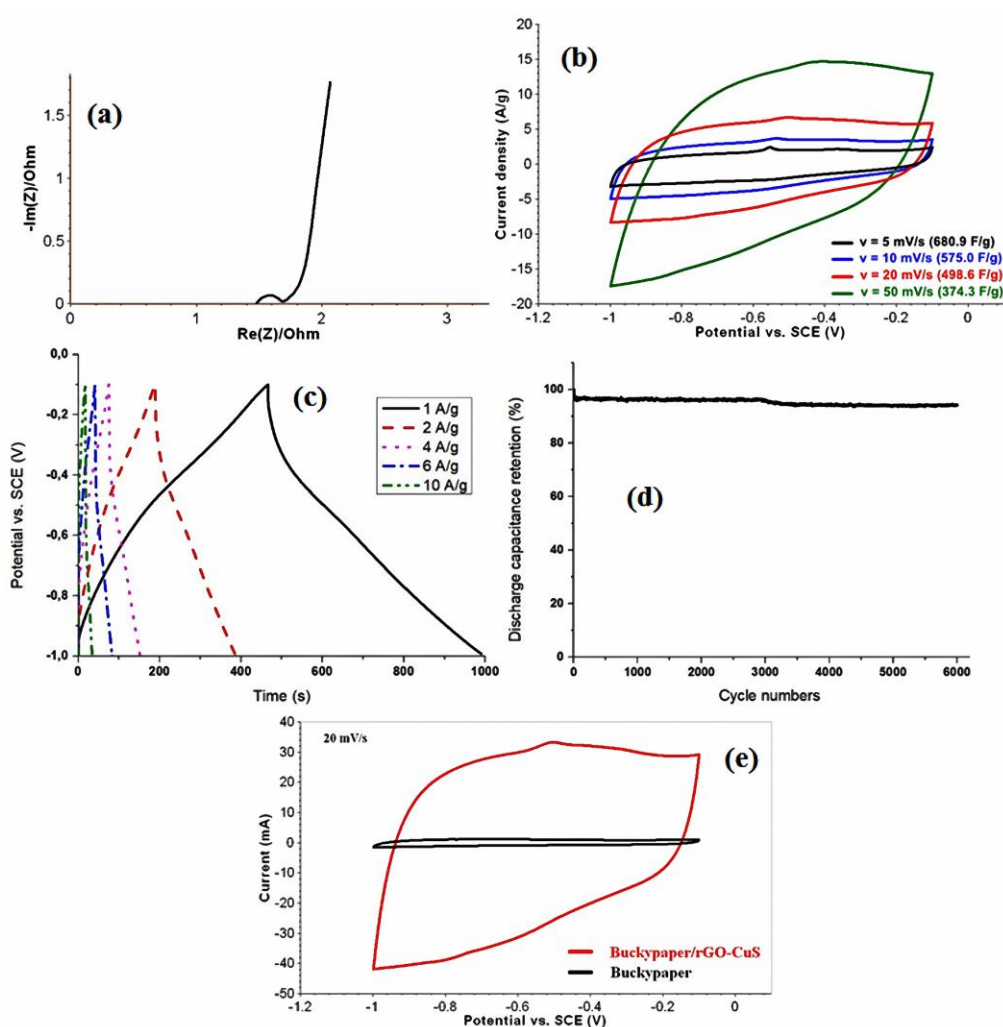


Figure 6. (a) EIS, (b) CV curves with various scan rates, (c) GCD curves with different current densities, (d) Percent capacitance retention after 6000 cycles of rGO-CuS SC electrode, and (e) CV curves of BP and rGO-CuS/BP SC electrode at scan rate of 20 mV/s.

Figure 6b shows the CV curves of the rGO-CuS electrode at different scan rates of 5, 10, 20, and 50 mV/s. The specific capacitance ( $C_s$ ) of the tested SC electrodes is calculated from the CV curves using the formula:

$$C_s = \frac{\int_{V_a}^{V_b} i(V)dV}{v \times m \times |V_b - V_a|} = \frac{S}{v \times m \times \Delta V} \quad (1)$$

where S is the area of the CV curve, v is the rate of change of potential over time, m is the mass of the rGO-CuS active material in the working electrode (if the vertical axis of the cv curve is the current density, m is ignored because the current density includes m), and ΔV is the working potential window (from -1 V to -0.1 V).

The specific capacitance values obtained are 680.9, 575.0, 498.6 and 374.3 F/g at scan rates of 5, 10, 20 and 50 mV/s, respectively. The specific capacitance values are high, commensurate with many recent publications [28 - 30]. Besides, the pseudo-capacitance effect can be seen on the CV curves through the redox peaks. Since CuS NPs account for only about 15 % of the active material's weight, the redox peaks are not so dominant. The double-layer charge effect of rGO still contributes most of the capacitance value.

Similar to the CV curves, the charging and discharging curves are also nonlinear lines (not straight lines) exhibiting the Faradaic effect (Fig. 6c). With a low current density of 1 A/g, the working time of the rGO-CuS electrode is up to 1000 seconds per cycle. And the electrode still responds well to current densities above 10 A/g. In Fig. 6d, the rGO-CuS/BP electrode was repeatedly charged and discharged for 6000 cycles at a current density of 25 A/g. After 6000 duty cycles, the electrode still maintains 94.3 % of its original capacity. Thus, due to the combination with rGO, the electrode durability is improved compared to supercapacitor electrodes containing only metal sulfide materials [21, 29]. Besides the electrochemical results of the fabricated supercapacitor electrode, we also performed a comparison of the capacitance of MWCNT Buckypaper and the printed rGO-CuS electrode. The results show that BP only contributes to the double-layer capacitance, and this capacitance is much smaller than that of the rGO-CuS/buckypaper electrode (Fig. 6e). This is consistent with the relatively smooth and hydrophobic surface of BP.

#### 4. CONCLUSIONS

Buckypaper has been successfully made by vacuum filtration with high solids content. At the same time, printing ink containing components of rGO and CuS nanoparticles has also been made suitable for printing technology. Thanks to the good dispersion of the ink and the heat treatment of the printed sample, a supercapacitor electrode with excellence electrochemical quality was produced. High capacitance value has been achieved at 680.9 F/g with a scan rate of 5 mV/s. The pseudo-capacitive effect occurs in both CV and GCD processes. In particular, after 6000 working cycles with an impressive current density of 25 A/g, the supercapacitor electrode still maintains a stability of 94.3 %. Thus, the technology of making rGO-NPs printing ink and Buckypaper could point us towards flexible supercapacitors and portable wearable devices.

**Acknowledgements.** This work was financially supported by [Institute for Tropical Technology](#) (2022 annual project).

**CRedit authorship contribution statement.** [Doan Thanh Tung](#) prepared Buckypaper. [Le Thi Thanh Tam](#) synthesized CuS nanoparticles. [Hoang Tran Dung](#) printed supercapacitor electrodes. [Ngo Thanh Dung](#) performed material analysis. [Doan Thanh Tung](#) and [Nguyen Thi Yen](#) performed electrochemical measurements. [Ngo Ba Thanh](#) supported for experiments. [Le Trong Lu](#) designed and guided experiments and supervised the project. All the authors read and approved the final manuscript.



**Declaration of competing interest.** The authors declare that they have no known competing financial interests or personal relationships that could have appeared to influence the work reported in this paper.

## REFERENCES

1. Iijima S. - Helical microtubules of graphitic carbon, *Nature*. **354** (1991) 56-58. <https://doi.org/10.1038/354056a0>.
2. Collins P. G., Avouris P. - Nanotubes for electronics, *Sci. Am.* **283**(6) (2000) 62-9. DOI: 10.1038/scientificamerican1200-62.
3. Balandin A. A. - Thermal properties of graphene and nanostructured carbon materials, *Nat. Mater.* **10** (8) (2011) 569-81. <https://doi.org/10.1038/nmat3064>.
4. Ibrahim K. S. - Carbon nanotubes-properties and applications: a review, *Carbon Letters* **14** (3) (2013) 131-144. <https://doi.org/10.5714/CL.2013.14.3.131>.
5. Byrne M. T. and Gun'ko Y. K. - Recent advances in research on carbon nanotube-polymer composites, *Advanced Materials* **22** (15) (2010) 1672-1688. <https://doi.org/10.1002/adma.200901545>
6. Amrollahi A., Rashidi A. M., Meibodi M. E., Kashefi K. - Conduction heat transfer characteristics and dispersion behaviour of carbon nanofluids as a function of different parameters, *J. Exp. Nanosci.* **4** (4) (2009) 347-63. <https://doi.org/10.1080/17458080902929929>.
7. Andrews R., Weisenberger M. C. - Carbon nanotube polymer composites, *Current Opinion in Solid State and Materials Science* **8** (1) (2004) 31-37. <https://doi.org/10.1016/j.progpolymsci.2009.09.003>.
8. Spitalsky Z., Tasis D., Papagelis K., and Galiotis C. - Carbon Nanotube-Polymer Composites: Chemistry, Processing, Mechanical and Electrical Properties, *Progress in Polymer Science* **35** (3) (2010) 357-401. <https://doi.org/10.1016/j.progpolymsci.2009.09.003>.
9. Patel M. D., Cha E., Choudhary N., Kang C., Lee W., Hwang J. Y., and Choi W. - Vertically oriented MoS<sub>2</sub> nanoflakes coated on 3D carbon nanotubes for next generation Li-ion batteries, *Nanotechnology* **27** (2016) 495401. <https://doi.org/10.1088/0957-4484/27/49/495401>.
10. Tan S. C., Li J. J., Zhou L. J., Chen P., Shi J. T. and Xu Z. Y. - Modified carbon fiber paper-based electrodes wrapped by conducting polymers with enhanced electrochemical performance for supercapacitors, *Polymers*. **10** (2018) 1072. <https://doi.org/10.3390/polym10101072>.
11. Sun C., Li X., Cai Z. S., and Ge F. Y. - Carbonized cotton fabric in-situ electrodeposition polypyrrole as high-performance flexible electrode for wearable supercapacitor, *Electrochim. Acta*. **296** (2019) 617-626. <https://doi.org/10.1016/j.electacta.2018.11.045>.
12. Zhang X. L., Lin Q. L., Zhang X. Q. and Peng K. P. - A novel 3D conductive network-based polyaniline/graphitic mesoporous carbon composite electrode with excellent electrochemical performance, *J. Power Sources* **401** (2018) 278-286. <https://doi.org/10.1016/j.jpowsour.2018.08.091>.
13. Zhu C., Mu X., Van A. P. A., Maier J., and Yu Y. - Fast Li storage in MoS<sub>2</sub>-Graphene-Carbon nanotube nanocomposites: advantageous functional integration of 0D, 1D, and 2D

- nanostructures, *Adv. Energy Mater.* **5** (2015) 1401170. <https://doi.org/10.1002/aenm.201401170>.
14. Popov K. M., Arkhipov V. E., Kurennya A. G., Fedorovskaya E. O., Kovalenko K. A., Okotrub A. V., Bulusheva L. G. - Supercapacitor performance of binder-free buckypapers from multiwall carbon nanotubes synthesized at different temperatures, *Phys. Status Solidi B* **253** (2016) 2406-2412. <https://doi.org/10.1002/pssb.201600240>.
  15. Susantyoko R. A., Parveen F., Mustafa I., Almheiri S. - MWCNT/activated-carbon freestanding sheets: a different approach to fabricate flexible electrodes for supercapacitors, *Ionics*. **25** (2019) 265-273. <https://doi.org/10.1007/s11581-018-2585-4>.
  16. Yi-Hsuan L., Shivam G., Chung-Hsuan H., Chi-Young L., Nyan-Hwa T. – Multilayered nickel oxide/carbon nanotube composite paper electrodes for asymmetric supercapacitors, *Electrochimica Acta*. **354** (2020) 136744. <https://doi.org/10.1016/j.electacta.2020.136744>.
  17. Wang X., Wei H., Liu X., Du W., Zhao X., Wang X. - Novel three-dimensional polyaniline nanothorns vertically grown on buckypaper as high-performance supercapacitor electrode, *Nanotechnology*. **30** (2019) 325401-325408. DOI: 10.1088/1361-6528/ab156d.
  18. Iurchenkova A. A., Fedorovskaya E. O., Asanov I. P., Arkhipov V. E., Popov K. M., Baskakova K. I., Okotrub A. V. - MWCNT buckypaper/polypyrrole nanocomposites for supercapacitor application, *Electrochimica Acta*. **335** (2020) 135700. <https://doi.org/10.1016/j.electacta.2020.135700>.
  19. Le T. T. T., Doan T. T., Ngo T. D., Phan N. H., Pham V. H., Phan N. M., and Le T. L. - Synthesis and Electrochemical Characterization of NiCo<sub>2</sub>S<sub>4</sub> Nanosheets/reduced Graphene Oxide for Energy Storage Applications, *Communications in Physics* **30** (4) (2020) 399. <https://doi.org/10.15625/0868-3166/30/4/15448>.
  20. Tung D. T., Dung H. T., Dung N. T., Hong P. N., Nguyen H. M., Van-Quynh N., Van Chuc N., Trung V. Q., Lu L. T., Minh, P. N. - Freeze gelation 3D printing of rGO-CuCo<sub>2</sub>S<sub>4</sub> nanocomposite for high-performance supercapacitor electrodes. *Electrochimica Acta*. **392** (2021) 138992. <https://doi.org/10.1016/j.electacta.2021.138992>.
  21. Ha M. Nguyen, Le T. T. Tam, Doan T. Tung, Nguyen T. Yen, Hoang T. Dung, Ngo T. Dung, Phan N. Hong, Le A. Tuan, Phan N. Minh and Le T. Lu - Facile synthesis of MnCo<sub>2</sub>S<sub>4</sub> nanosheets as a binder-free electrode material for high performance supercapacitor applications, *New J. Chem.* **46** (2022) 13996-14003. <https://doi.org/10.1039/D1NJ05809F>.
  22. Thanh Tam L. T., Tung D. T., Nguyen H. M., Ngoc Linh N. T., Dung N. T., Van Quynh N., Van Dang N., Vernardou D., Le T. K., Tuan L. A., Minh P. N., Lu L. T. - High electrochemical performance of ink solution based on manganese cobalt sulfide/reduced graphene oxide nano-composites for supercapacitor electrode materials, *RSC Adv.* **12** (31) (2022) 20182-20190. <https://doi.org/10.1039/D2RA02818B>.
  23. Tam Le T. T., Hung N. V., Tung D. T., Dung N. T., Dung H. T., Nam P. T., Minh P. N., Hong P. N., Lu L. T. - Synthesis and electrochemical properties of porous CNTs-Ferrite hybrid nanostructures for Supercapacitor, *Vietnam J. Sci. Technol.* **57** (2019) 58. <https://doi.org/10.15625/2525-2518/57/1/12801>.
  24. Tung D. T., Tam Le T. T., Dung H. T., Dung Ngo T., Dung Nguyen T., Hoang Thai, Lam T. D., Minh P. N., Thu T. V., Hong P. N., Lu L. T. - Direct Ink Writing of Graphene–Cobalt Ferrite Hybrid Nanomaterial for Supercapacitor Electrodes, *J. Electron. Mater.* **49** (2020) 4671. <https://doi.org/10.1007/s11664-020-08165-z>.

25. Oliveira A. E. F., Braga G. B., Tarley C. R. T., Pereira A. C. - Thermally reduced graphene oxide: synthesis, studies and characterization, *J. Mater. Sci.* **53** (2018) 12005-12015. <https://doi.org/10.1007/s10853-018-2473-3>.
26. Htwe Y. Z. N., Abdullah M. K., Mariatti M. - Effect of sodium dodecyl concentration on the properties of graphene conductive inks, *Materials Today: Proceedings* **66** (5) (2022) 2836-2839. <https://doi.org/10.1016/j.matpr.2022.06.525>.
27. Ersin Y., Mehmet D., Yasemin T. - Effect of sodium dodecyl sulfate on thermal properties of polyvinyl alcohol (PVA)/modified single-walled carbon nanotube (SWCNT) nanocomposites, *Diamond and Related Materials* **115** (2021) 108359.
28. Kalyan Ghosh and Suneel Kumar Srivastava - Enhanced Supercapacitor Performance and Electromagnetic Interference Shielding Effectiveness of CuS Quantum Dots Grown on Reduced Graphene Oxide Sheets, *ACS Omega* **6** (7) (2021) 4582-4596. <https://doi.org/10.1021/acsomega.0c05034>.
29. Heydari H., Moosavifard S. E., Shahraki M., Elyasi S. - Facile synthesis of nanoporous CuS nanospheres for high-performance supercapacitor electrodes, *Journal of Energy Chemistry* **26** (4) (2017) 762-767. <https://doi.org/10.1016/j.jechem.2017.03.007>.
30. Soliman I. El-Hout, Saad G. Mohamed, Amira G., Sayed Y. Attia, Ahmed S., Said M. El-Sheikh - High electrochemical performance of rGO anchored CuS nanospheres for supercapacitor applications, *Journal of Energy Storage* **34** (2021) 102001. <https://doi.org/10.1016/j.est.2020.102001>.